Accepted in Solar Energy with minor revision (under-review)

Solar radiation estimation at high latitudes: Assessment of the CMSAF databases, ASR and ERA5

Bilal Babar*, Rune Grand Graversen and Tobias Boström

Department of Physics and Technology, The Arctic University – University of Tromsø, Norway

*corresponding author: bilal.babar@uit.no

Abstract

There is a growing demand for the estimation of solar energy potential at high latitude locations. This study compares four datasets; Cloud, Albedo, Radiation dataset Edition 2 (CLARA), Surface Solar Radiation dataset – Heliosat Edition 2 (SARAH), ECMWF Reanalysis 5 (ERA5) and Arctic System Reanalysis v2 (ASR) on high latitude locations. Global horizontal irradiance (GHI) from these datasets is compared with *in-situ* ground-measurements over multiple locations in Norway. The first two datasets are mainly based on satellite estimation of solar radiation, while the latter two are based on a combination of a weather-prediction model, satellite data, and other observations. The datasets are evaluated against quality-controlled *in-situ* measurements of solar radiation from pyranometers. Overall, CLARA, SARAH, and ERA5 show moderate errors, while those of ASR are considerably larger. Monthly averages of global horizontal irradiance have mean absolute deviation (MAD) of 6.3 Wm^{-2}, 5.8 Wm^{-2}, 6.4 Wm^{-2}, and 14.5 Wm^{-2} for CLARA, SARAH, ERA5, and ASR, respectively. Seasonal error analysis of these datasets reveals that SARAH has the lowest errors in all seasons. The datasets are classified into clear-sky, intermediate-cloudiness, and overcast categories, by using two thresholds of cloudiness based on the ratio of radiation at ground to its corresponding clear-sky value (clear-sky index). The categories obtained from satellite and reanalysis data are then compared against estimates based on corresponding *in-situ* observations; this analysis shows that both CLARA and SARAH perform better than ERA5 and ASR for these categories. SARAH and CLARA perform similarly in all types of conditions, but a gradual increase in errors for an increase of cloudiness is observed for ERA5 and ASR. Yearly energy analysis shows that CLARA performs better than other datasets for locations above latitude 65ºN, and SARAH performs better in locations below 65ºN. A further analysis is performed to assess the cloud sensing abilities of ERA5. On a shorter time scale, there are errors due to inaccurate representation of clouds, however on longer time scales *i.e.* months and years, these errors are considerably reduced. ERA5 is observed to overestimate TCWC (the total cloud water content defined as the mass of water and ice in a cloud) in clear-sky and intermediate-cloudy categories, while in overcast category it is underestimated. Generally, an overestimation of solar radiation is observed in reanalysis and an underestimation is observed in satellite methods.

Keywords: Solar radiation, Arctic, Reanalysis, Satellite estimations, CMSAF, ECMWF

1. Introduction

Accurate solar resource measurements at potential photovoltaic (PV)/thermal installation sites are usually not available. For example, only a few meteorological stations record high-quality measurements in Norway (Øyvind et al., 2013). The assessment of solar resource at a specific location forms the basis for future installations. However, solar radiation is intermittent in nature and its variation on longer times scales is important for the planning of future installations (Crabtree et al., 2011). In addition, such information is also used in the long and short-term forecasting of power production and in optimizing energy dispatch strategies (Heinemann et al., 2006; Remund et al., 2008). Long time series of global horizontal irradiance (GHI) is used in the energy sector as well as in meteorology, agriculture, and climate studies.

The three main components to consider before installing a solar energy system are site selection, annual output and temporal performance/operating strategy. These components are directly related to the resource potential of the site, and can be evaluated by analysing long-term historical data series. Often a typical meteorological year (TMY), which is derived from the historical data *e.g.* within the past 30 years, is used to assess site locations for feasibility (Hall et al., 1978). Recent studies like those of Huld et al. (2018) and Stoffel et al. (2010) have shown that TMY is not a good indicator for predicting solar radiation for a given year, but rather it represents typical estimates of the average long-term conditions. Sufficiently long historical records from ground-measurements are seldom available for a given location for constructing a reliable TMY. Therefore satellite estimations and reanalyses provide an alternative to the ground-measurements for these estimations (Stoffel et al., 2010).

Estimating surface solar radiation from the visible spectrum of sensors installed on satellites is a well-developed procedure (Cano et al., 1986; Gautier et al., 1980; Rigollier et al., 2004; Tarpley, 1979). However, the accuracy of these methods is lower than ground measurements, but the advantages of the satellite methods include large spatial and temporal coverage (Noia et al., 1993). Surface solar radiation estimated from geostationary satellites provide up to sub-hourly values on a few km grid resolution, while polar orbiting satellites provide up to daily average solar radiation. All geostationary satellites have a limited spatial coverage because these are positioned over the equator at 0º. In the case of Meteosat First Generation (MFG) and Meteosat Second Generation (MSG) geostationary satellites, they have a coverage of ±65º in latitude and longitude. At latitudes higher than these, they encounter a flat angle of view that decreases the spatial resolution and increases errors. Alternatively, polar orbiting satellites can be used at high-latitude locations, as they provide almost global coverage. The main shortcoming of polar orbiting satellites is low sensing frequency, which varies from twice daily at the equator to 14 times a day near poles (Pinker and Laszlo, 1992; Platt, 1983). Satellite-based solar radiation-estimation methods have high accuracy, but some studies like that of Gueymard (2011) and Ineichen (2014) have shown that large errors may exist. For uncertainties and known issues within the satellite-based solar radiation estimation techniques see Suri and Cebecauer (2014).

In Earth System Models (ESM) or reanalysis, solar radiation is often referred to as down-welling surface shortwave flux. There are a number of studies where reanalyses have been used to estimate solar radiation and power (Boilley and Wald, 2015; Juruš et al., 2013; Wild et al., 2015). However, an increase in bias with increasing latitude was observed in one of the studies (Yi et al., 2011). The main advantages of reanalyses include multi-decadal time series, worldwide coverage, and free-of-cost availability. Recently, it has been found that reanalysis-based irradiance estimates can be a useful supplement when satellite irradiance is not available (Bojanowski et al., 2014; Urraca et al., 2018), although, many studies have reported overestimations in reanalysis (Boilley and Wald, 2015; Kennedy et al., 2011; Wild, 2008).

The aim of this paper is to analyse four different datasets regarding their accuracy and provide a comparative analysis for high-latitude conditions. Two of these are based on satellite methods, a polar orbital Cloud, Albedo, Radiation dataset Edition 2 (CLARA 2), and a geostationary Surface Solar Radiation dataset – Heliosat Edition 2 (SARAH 2). The other two are based on a combination of a weather-prediction model and various types of observations; a global reanalysis; ECMWF Reanalysis 5 (ERA5), and a dynamical downscaling of such a reanalysis (ERA-interim); Arctic System Reanalysis v2 (ASRv2). The analysis is performed for Norway, which represents a complex topography and a large variation in latitudes ranging from 59º to 70ºN. Previously, CLARA-A1 and CLARA-A2 datasets have been compared for multiple locations in Norway and Sweden (Babar et al., 2018). It was found that the new edition of CLARA has less number of missing data points. However, CLARA-A2's new data points, which previously were missing in CLARA-A1, have high errors. These points mostly lie in the high latitude locations where a snow cover is frequent. Because of the difficulties in differentiating snow covers from clouds, such errors exist. Here we extend this work and the novelty lies in evaluating the above-mentioned datasets for GHI for high-latitude locations and providing an analysis of these datasets in different conditions. The datasets are evaluated for daily means, monthly means, yearly means, seasonal analysis, energy analysis, and performance in different sky categories. Daily and monthly averages are evaluated by dividing the locations in four groups, including above 65ºN, below 65ºN, coastal and inland regions. In the final section, the effects of clouds in ERA5 are computed for different sky categories and compared with ground-measured solar radiation, which gives an insight into the challenges of estimating solar radiation in ERA5.

This paper is formatted as follows: Section 2 gives a description of the datasets analysed in this study. Section 3 provides an overview of the quality control procedures applied on the ground data and validation metrics. Section 4 presents the results and provides a brief discussion. Section 5 concludes the findings of this work.

2. Datasets

The datasets analysed in this study have different spatial and temporal resolution. Table 1 shows an overview of the datasets. SARAH and ASR can be considered as high-resolution datasets, while CLARA and ERA5 are coarse resolution datasets. SARAH is the highest resolution dataset with hourly temporal resolution and a spatial resolution of 0.05ºx0.05º. ASR contains data with three-hour temporal resolution and a spatial resolution of 15 km (0.136º). For both of these datasets, the nearest grid point from the site location is selected for data extraction. However, CLARA and ERA5 provide data on a much coarser grid of 0.25ºx0.25º and 0.28ºx0.28º, respectively. Data extraction from these datasets is performed by selecting the four surrounding grid points at site locations and applying inverse weighted-distance interpolation to obtain solar radiation at the coordinates of the site. In case of

CLARA, there are missing data points, which imply that at some of the periods there are no available data in the surrounding four points. When the surrounding points have less than three valid values, the interpolation is replaced by a missing value indicating that no valid values exist at that particular time and place. ASR and ERA5 do not contain missing values.

The datasets used in this study have certain spatial and temporal limitations. SARAH is limited to ±65º in latitude and longitude due to the shape of the viewing disc of MFG/MSG satellites and because of the flat viewing angle of geostationary satellites that results in increased errors above 65ºN. The evaluation of SARAH dataset is performed for locations below 65ºN latitude. CLARA and ERA5 are global datasets, whereas ASR is regional but covers all locations analysed in this study. SARAH and CLARA are available from 1983 to 2015 and 1982 to 2015, respectively. At the time of writing, ERA5 is available from 2000 to 2017. The years from 2000 to 2015 are included in this study from these datasets. ASRv2 is available from 2000 to 2012 and its complete available time series is used.

Table 1

Description of the datasets used in this study. The period analysed, spatial and temporal resolutions are shown for each dataset.

	Method	Years analysed	Spatial resolution	Highest temporal resolution	Spatial limits
CLARA -A2	Polar-orbiting Satellite	2000-2015	0.25ºx0.25º	24 Hours	Global
SARAH -2	Geostationary Satellite	2000-2015	0.05ºx0.05º	0.5 Hour	Limited to ±65º latitude and ±65º longitude
ERA5	Reanalysis (Global)	2000-2015	0.281ºx0.281º	1 Hour	Global
ASRv2	Reanalysis (Regional renalaysis downscaled from ERA-interim)	2000-2012	0.136ºx0.136º	3 Hours	180W - 180E longitude 24.643N - 90N latitude

2.1 CLARA-A2

The CLARA-A2 dataset was released in December 2016 and it is the second edition of CLARA (Cloud, Albedo, Radiation dataset) by satellite application facility on climate monitoring (CM-SAF). The dataset is available from 1 January 1982 to 31 December 2015, and constitutes an extension of 6 years relative to the previous CLARA-A1 dataset. This dataset has global coverage with a spatial resolution of 0.25ºx0.25º on a regular lat-lon grid and it provides daily and monthly averages of surface incoming shortwave radiation (SIS). To calculate daily averages, at least 20 observations of incoming solar radiation in each grid box are required; similarly, 20 valid daily averages are required to generate monthly averages (Trentmann and Kothe, 2016). Along with SIS, CLARA also provides longwave up and down-welling surface radiation.

The fundamental method used in calculating surface solar irradiance from satellite observations is based on the reflectance measured by the satellite instruments, which is related to the atmospheric transmittance. The underlying algorithm in CLARA uses the Advanced Very High Resolution Radiometer (AVHRR) sensor data to derive the atmospheric transmittance, which is used in calculating surface incoming solar radiation. The solar radiation is estimated by using the solar zenith angle, cloud coverage, vertically-integrated water vapour, and aerosol optical depth. Finding solar zenith angles is straightforward and can be calculated accurately. The vertically-integrated water vapour and aerosol optical depth are not available in the AVHRR data and for these fields, external sources are used. For vertically-integrated water vapour, ERA-Interim Reanalysis (Dee et al., 2011) is used and the vertical ozone column is set to a constant value of 335 DU, as its variability has negligible impact on the estimated solar radiation. Aerosol information is taken from the modified version of the monthly mean aerosol fields from Global Aerosol Data Set/ Optical Properties of Aerosols and Cloud (GADS/OPAC) climatology. In the algorithm, AVHRR data is used to retrieve only the cloud cover information. The first step in estimating surface solar radiation is the classification of the sky condition. The Nowcasting SAF (SAFNWC) software is used to derive the information on cloud coverage for each pixel by using the information from the satellite sensors. If no cloud is detected (cloud free pixel), surface solar radiation is calculated by using the clear-sky Mesoscale Atmospheric Global Irradiance Code (MAGIC) by using only auxiliary sources. If the pixel is classified as cloudy (cloud contaminated or fully cloudy), visible channels of AVHRR instrument are used to derive broadband reflectance. These reflectances are then transferred to broadband fluxes by using a bidirectional reflectance distribution function (BRDF). In the next step, these broadband top-of-the-atmosphere albedos are used to derive transmissivity through a look-up table approach. Finally, the transmissivity is used in calculating surface solar radiation. In this

dataset, all data points with a solar zenith angle larger than 80º are set to missing values and solar zenith angle larger than 90º is set to zero. However, because a temporally constant surface albedo is used in the algorithm, this dataset does not provide radiation estimates on snow and sea ice coverage areas because changes in the albedo of the snow-covered surfaces are not considered (Karlsson et al., 2017). High-latitude locations may have a very different surface albedo than the temporally constant albedos considered in the algorithm. Such grid points are identified by calculating the difference between monthly mean CLARA-A2 SAL (surface albedo) data record and the surface albedo used in the processing of SIS. These critical grid points, which have a difference in surface albedo exceeding 35%, are masked-out from the final product by setting them as missing values. For more information on the CLARA dataset and its accuracy refer to Karlsson et al. (2017).

2.2 **SARAH-2**

The second version of surface solar radiation dataset – Heliosat (SARAH-2) is a climate data record of surface solar radiation by CMSAF (Pfeifroth et al., 2017a) and covers a period of 32 years from 1983 to 2015 and the region from 65ºN to 65ºS latitude and 65ºW to 65ºE longitude. The spatial resolution of the data is 0.05ºx0.05º (approximately 5km) and the data is available for 30 minutes instantaneous, hourly, daily, and monthly averages of surface incoming shortwave radiation on a horizontal surface, direct normal irradiance (DNI) and effective cloud albedo (CAL). To calculate daily averages at least three samples per day are required; similarly, 10 existing daily averages are required to generate monthly averages.

In this dataset, the broadband visible channels from Meteosat Visible Infra-Red Imager (MVIRI) instrument on-board the Meteosat first generation satellites and the Spinning Enhanced Visible and Infrared Imager (SEVIRI) instruments on-board the Meteosat second generation satellites are used to calculate the shortwave surface radiation. In the first step, the effective cloud albedo (CAL) is retrieved from the satellite data by using a modified Heliosat method (Hammer et al., 2003). This modification of the Heliosat method in combination with gnu-MAGIC/SPECMAGIC is called MAGICSOL. The modified Heliosat method provides the broadband effective CAL, but to consider the spectral effect of clouds, a Radiative Transfer Model (libRadtran) based correction is applied. The CAL is related to the cloud transmission and, hence, by calculating clear-sky radiation, the all-sky radiation can be estimated. In this dataset, for calculating clear-sky radiation the SPECMAGIC model is used, which is based on a so-called hybrid eigenvector look-up table approach (Mueller et al., 2012). The input parameters for gnu-MAGIC/SPECMAGIC are date, time, solar zenith angle, coordinates, effective cloud albedo (cloud index), water vapour column density, surface albedo, aerosol optical thickness, and single scatter albedo for aerosols. Monthly mean values of vertically-integrated water vapour are taken from ERA-interim global reanalysis record (Dee et al., 2011), and monthly mean aerosol information is taken from Monitoring Atmospheric Composition and Climate project (MACC) aerosol climatology. Surface solar radiation is derived from combining the SPECMAGIC algorithm and the effective cloud albedo (Pfeifroth et al., 2017b). One of the limitation of SARAH is that for solar zenith angles between 88º and 90º, the corresponding data points are set as missing values, and above solar zenith angle of 90º, the data points are set to zero. Improvements in the new version of the dataset includes stability during the change of instrument from MVIRI to SEVIRI in 2006, and correction of the cloud albedo to account for the slant viewing geometry effects (Pfeifroth et al., 2018). For more information on the retrieval methods refer to Müller et al. (2015).

2.3 ERA5

ECMWF Reanalysis 5 (ERA5), is the fifth generation of European Centre for Medium-Range Weather Forecasts (ECMWF) atmospheric reanalysis of the global climate and span a period of 1950 to near real time (Hans and Dick, 2016). At the time of this study, data from 2000 to 2017 are available. Further data back in time will be released in 2019-20 and will continue to update forward in real-time. In ERA5, the solar radiation variable has a spatial resolution of 31km (0.28125ºx0.28125º) and an hourly temporal frequency. ERA5 uses the Integrated Forecasting System (IFS) cycle 41r2 with a state-of-the-art four-dimensional variational analysis (4DVAR) assimilation system. ERA5 has more pressure levels than ERA-Interim (the previous edition of ECMWF reanalysis) and more variables are made available for this reanalysis than for those of earlier generation. For more information on ERA5 refer to ECMWF (2018).

In this study, shortwave surface downward radiation, shortwave surface downward radiation clear-sky, and total cloud water content (the vertically-integrated cloud water concentration) are used from this dataset. In ERA5, the incoming short wave radiation is obtained from a Radiative Transfer Model (RTM). This model simulates the attenuation in solar radiation caused by the atmosphere, therefore, the quality of estimated radiation depends on

the RTM used. Reanalysis generally do not assimilate aerosol, clouds or water vapour data, which increases the uncertainty in the estimated surface irradiance (You et al., 2013; Zhao et al., 2013).

2.4 Arctic System Reanalysis v2

Arctic system reanalysis version 2 (ASRv2) is a polar-optimized dynamic downscaling of ERA-Interim reanalysis by using Weather Research and Forecast Model (WRF) version 3.6.0. The data set is available for the period of 2000 to 2012. The grid resolution is 15km, which is finer than most global models and the previous release of ASR (ASRv01), whereas the time resolution of the dataset is 3 hours. The downscaling is optimized for Polar Regions, and polar physics is used where possible, including heat transfer through snow and ice, the fractional sea ice cover, the ability to specify variable sea ice thickness, snow depth on sea ice and sea ice albedo, as well as other optimizations included in the Noah Land Surface Model. The area covered by this dataset is 1.2×10^8 km^2, which is about 50% of Northern hemisphere. Spectral nudging from ERA-Interim is applied on geopotential height, temperature, and wind components above 100 hPa on the inner domain. ASR uses three-dimensional variational analysis (3DVAR) for observations, including radiance data, from a number of satellites (Bromwich et al., 2017).

3. Ground data

In this study, 31 locations from Norway are analysed for the four mentioned datasets. The coordinates of the locations, altitudes, and land type are indicated in appendix A and an overview of site locations is shown in Figure 1. The ground-measured data is acquired from the Norwegian Institute of Bioeconomy Research (NIBIO). NIBIO registers hourly-average GHI by using Kipp and Zonen CMP11 or CMP13 pyranometers. The data is quality controlled and the equipment is maintained regularly on a daily or weekly basis (http://lmt.bioforsk.no/about). The daily averages of ground data were calculated by following Urraca et al. (2017b), where these were calculated for those days when at least 20 valid hourly means were available, however when this criteria was not met the daily average was replaced by a missing value. Similarly, the monthly averages were calculated for those months when all the hourly values were available. If this condition was not met, the monthly average was replaced by a missing value (Roesch et al., 2011). The amount of missing data in the ground measurement was largely reduced because of the application of quality control procedures (explained in the next section).

In this study, the numbers of years used from each data set are different. For ASR, 12 years of data is used and 16 years of data is used for ERA5, CLARA, and SARAH. Furthermore, the sites are divided four groups; above 65ºN, below 65ºN, inland and coastal regions. The studied locations are divided into coastal and inland regions are grouped by observing the proximity to the shoreline. Regions within 30 km of the shoreline are considered as coastal. From the 31 locations studied here, 14 sites are classified as coastal and 17 sites as inland, while 4 sites lie above 65ºN and 27 lie below 65ºN latitude. For details on the land-type classification, refer to appendix A.

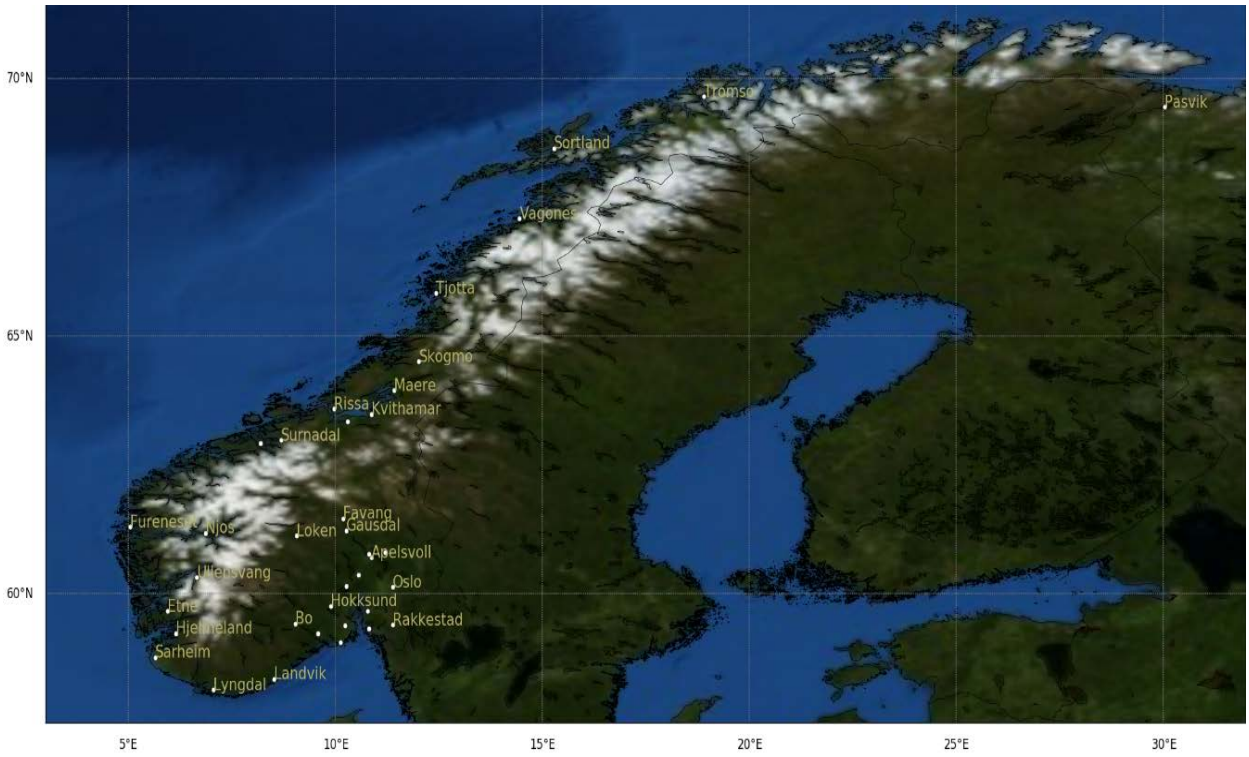

Figure 1: Locations of the sites included in the study. To avoid overlapping of names some locations are shown with only white dots.

3.1 Quality Control

Although the data provided by NIBIO is quality controlled, Urraca et al. (2017a) observed that operational and equipment errors exist in NIBIO stations. The first quality-control check performed in this study is to look at the percentage of missing data. Any year having more than 5% of missing values is discarded from the analysis. The second check is performed by using BSRN Global Network recommended Quality Control tests, V2.0 (Long and Dutton, 2010). These quality checks test values that are extremely rare and physically impossible. From this test, years having more than 1% of flagged values are removed from the ground data. The third quality control procedure is applied by using the Urraca et al. (2017a) quality control technique. In this test, CLARA and ERA5 datasets are used to check the quality of ground measurements by constructing confidence intervals to detect the operational and equipment errors. Following Urraca et al. (2017a), the locations in Norway are divided into two sections by grouping locations above 65ºN and locations below 65ºN. Separate confidence intervals are constructed for these groups of locations. After constructing these confidence intervals, the ground data is passed through an algorithm to check the data with errors, which appear in the form of flags. Following Urraca et al. (2017a) two checks are performed, one to see the operational errors and the other to see the equipment errors. After these checks, the years having large number of flags are visually inspected and removed from the analysis. Initially Pasvik, Mære, Njøs, and Ullensvang were included in the study but due to a large number of flags from the third quality control test, these were discarded. Pasvik and Ullensvang were found to have equipment errors and frosting, while Mære and Njøs were found to have shading errors. For more information on this quality control procedure refer to Urraca et al. (2017a). 2006 and 2007 were found to have a large number of missing data points; these were discarded from all locations. Gap filling methods are only used in calculating yearly energy averages by using nearest-neighbour interpolation. See appendix B for details about the years not included in the study. After performing quality control on the ground data, errors might still exist but in addition to validating the datasets, this study provides a comparative analysis of these datasets for high latitude locations. From a comparative point of view, the errors in the ground data will have a similar effect on all datasets.

3.2 Validation

In order to evaluate the performance of the datasets, some common statistical measures are used. The most widely used measure is the root mean square deviation (RMSD). As an addition, the BIAS or mean bias deviation (MBD) is used in the evaluation. MBD gives an insight in under or over estimations. Mean absolute deviation (MAD) is

also used for the evaluations. Because of the absolute values used in this measure, the negative and positive errors do not cancel out as in the BIAS. MAD is a good measure for comparing different models. Moreover, Pearson correlation and scatter plots are used to indicate the spread and overall correlation of the datasets with ground measurements.

4. Results and discussion

Table 2 lists the RMSD, MAD, and MBD of the datasets for the locations included in the study. The error indicators in table 2 are expressed in Wm^{-2} and values in parentheses are daily averages. Night-time values are included in calculating daily and monthly averages. Along with all sites included in the study, table 2 also shows error metrics for above 65ºN, below 65ºN, inland and coastal regions.

Table 2
Error metrics expressed in Wm^{-2}, for the datasets analysed in this study. Numbers without parentheses are monthly averaged errors while those in parentheses are daily averaged errors. Numbers are averaged over all stations. Error metrics for different geographical groups are also shown.

	RMSD(Wm^{-2})				MAD(Wm^{-2})				MBD(Wm^{-2})			
	CLARA	SARAH	ERA5	ASR	CLARA	SARAH	ERA5	ASR	CLARA	SARAH	ERA5	ASR
All Sites	9.5 (18.3)	8.7 (18.0)	9.9 (26.4)	21.7 (42.6)	6.3 (12.8)	5.8 (11.8)	6.4 (16.7)	14.5 (27.1)	-3.0 (-1.7)	-3.6 (-2.5)	2.1 (4.0)	13.1 (16.9)
Above 65ºN	10.1 (16.0)	-	10.9 (26.3)	20.3 (39.4)	5.3 (9.7)	-	6.1 (14.5)	11.1 (21.5)	-3.4 (-2.8)	-	3.8 (5.6)	8.0 (11.0)
Below 65ºN	9.4 (18.6)	8.7 (18.0)	9.9 (26.8)	21.9 (43.0)	6.5 (13.2)	5.8 (11.8)	6.5 (17.3)	15.0 (27.9)	-3.0 (-1.5)	-3.6 (-2.5)	2.0 (4.0)	13.8 (17.8)
Coastal	9.1 (17.5)	8.5 (17.1)	10.0 (26.5)	21.8 (41.9)	5.9 (12.1)	5.6 (11.2)	6.2 (16.3)	13.9 (25.6)	-2.7 (-3.1)	-3.4 (-2.2)	2.3 (4.3)	11.9 (15.7)
Inland	9.3 (23.4)	8.8 (18.4)	10.0 (26.9)	21.7 (43.1)	6.2 (14.5)	5.9 (12.1)	6.7 (17.6)	15.0 (28.3)	-3.0 (-5.0)	-3.7 (-2.7)	2.2 (4.1)	14.0 (18.0)

From the table it can be seen that for all locations, SARAH provides the best estimation in terms of RMSD, while ASR performs the worst. The same pattern follows on the MAD errors where SARAH performs better than other datasets, while ASR has the highest errors. ERA5 and ASR (reanalysis models) are observed to be overestimating, similar to previous studies (Boilley and Wald, 2015; Kennedy et al., 2011; Wild, 2008). Both CLARA and SARAH (satellite databases) underestimate solar radiation (Posselt et al., 2012; Riihelä et al., 2015). At slant angles of view, such as those experienced by geostationary satellites at high latitudes, solar radiation is often underestimated by satellite methods because of an overestimation in cloud. The highest bias is seen in ASR while biases of CLARA, SARAH, and ERA5 are very similar in magnitude.

The table also shows RMSD, MAD, and MBD for location categories above 65ºN, below 65ºN, coastal and inland. Above 65ºN latitude, CLARA has the lowest errors and ASR has the highest errors while ERA5 provides moderate errors. SARAH does not provide coverage above 65ºN latitude. At locations below 65ºN, SARAH and CLARA have low errors as compared to other datasets. The ASR has the highest errors at such locations as well. SARAH and CLARA have lower errors in coastal regions than inland, mainly due to less snow covers in coastal regions (Babar et al., 2018). Note that CLARA and ERA provide data at a similar spatial resolution, i.e. 0.25º and 0.28º, however the surface radiation in CLARA is calculated at much finer resolution (around 4km) than in ERA5, therefore, CLARA performs better at coastal regions. On the contrary, in inland locations SARAH provides better estimates than other datasets. CLARA comes second in terms of both daily and monthly means, while ASR performs the worst. In this analysis, ERA5 is seen to perform better at locations below 65ºN than above 65ºN latitude.

Figure 2 (a-h) illustrates the scatter plots of the monthly and daily averages of the datasets. The black coloured line represents the x=y line for reference. Evidently, CLARA and SARAH have a very similar spread on both monthly and daily averages. A correlation of 0.98 for daily means and 0.99 for monthly means are observed for both of these datasets. ASR has a wider spread in scatter plots with correlation coefficients of 0.99 and 0.92 for monthly and daily means respectively. In addition, a positive bias in ASR monthly averages can be observed. ERA5 has an intermediate spread with a correlation of 0.99 for monthly averages and 0.95 for daily averages.

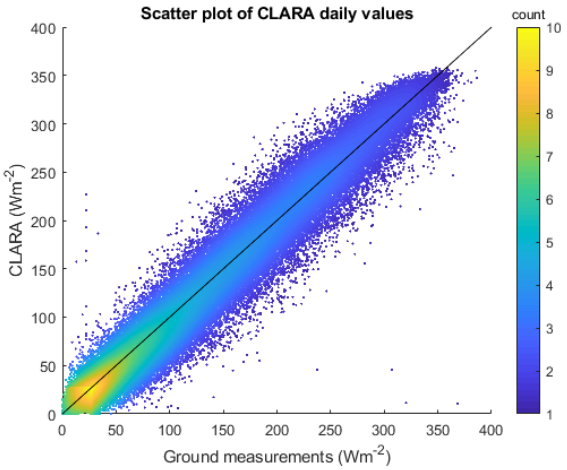
Scatter plot of CLARA daily values
CLARA (Wm-2)
Ground measurements (Wm-2)
count

(a)

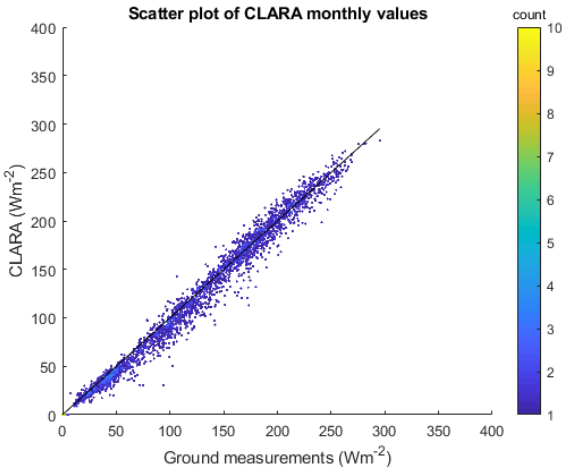
Scatter plot of CLARA monthly values
CLARA (Wm-2)
Ground measurements (Wm-2)
count

(b)

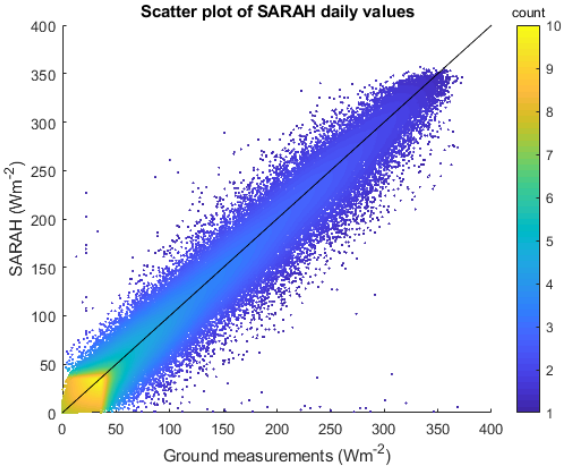
Scatter plot of SARAH daily values
SARAH (Wm-2)
Ground measurements (Wm-2)
count

(c)

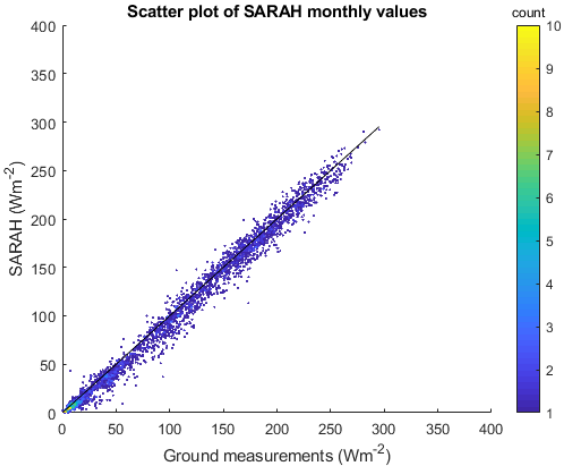
Scatter plot of SARAH monthly values
SARAH (Wm-2)
Ground measurements (Wm-2)
count

(d)

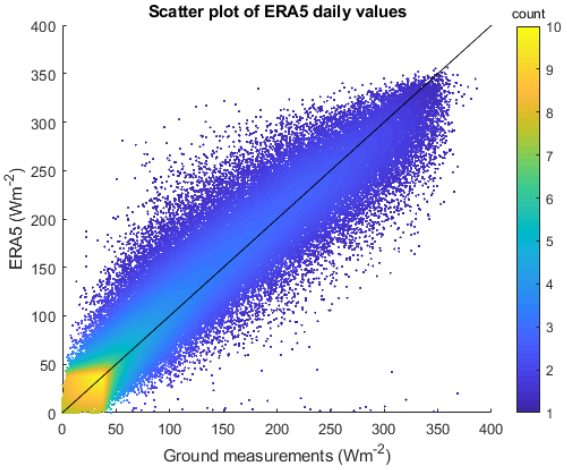
Scatter plot of ERA5 daily values
ERA5 (Wm-2)
Ground measurements (Wm-2)
count

(e)

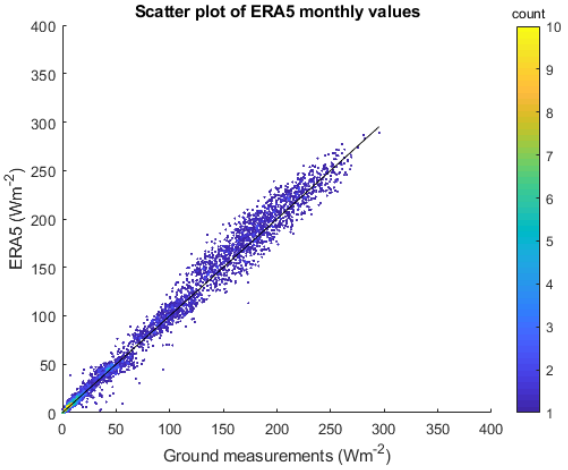
Scatter plot of ERA5 monthly values
ERA5 (Wm-2)
Ground measurements (Wm-2)
count

(f)

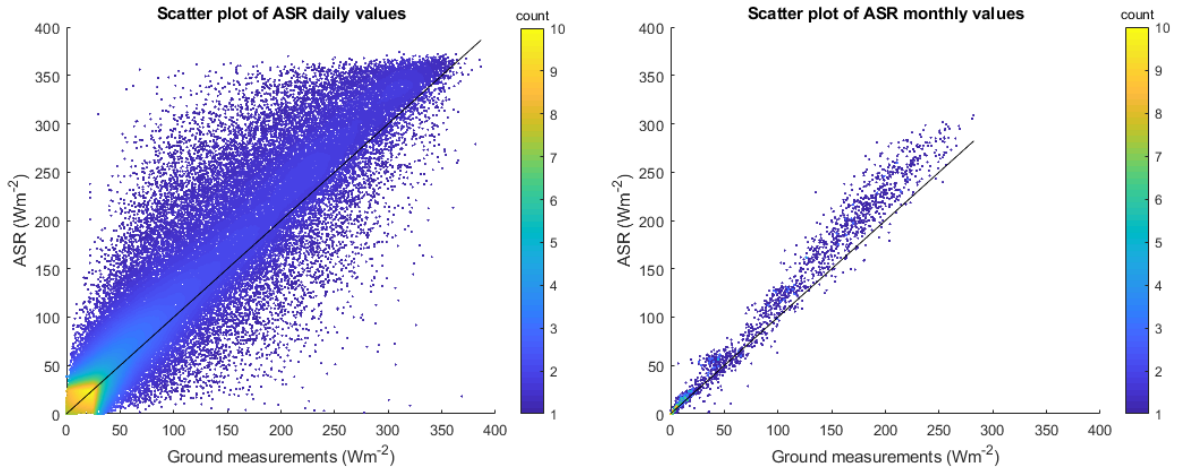

(g) (h)

Figure 2: Monthly mean and daily mean GHI scatter plots of the datasets. Ground *in-situ* observations and estimated values of solar radiation are given in Wm^{-2}. The legend bar shows the density of data points on a coloured scale. Satellite data show narrow spread and underestimation while reanalyses show wider spread and overestimation.

Table 3

Statistical errors of the yearly average energy estimates for the datasets in kWh per square meter and year on a horizontal surface. Energy statistics for different geographical groups are also shown.

	Energy ($KWh.m^{-2}.year^{-1}$/percentage error)											
	CLARA			SARAH			ERA5			ASR		
	Est.	Obs.	%Err.	Est.	Obs.	%Err.	Est.	Obs.	%Err.	Est.	Obs.	%Err.
All Sites	838.4	862.9	-2.8	861.2	880.5	-2.2	908.1	862.9	+5.2	1017.1	865.5	+17.5
Above 65ºN	711.7	715.5	-0.5	-	-	-	806.0	715.5	+12.6	870.4	751.3	+15.9
Below 65ºN	853.5	880.5	-3.1	861.2	881.2	-2.3	920.3	881.2	+4.4	1034.8	879.3	+17.7
Coastal	845.4	857.6	-1.4	882.2	899.9	-1.9	904.9	857.6	+5.5	1009.4	862.6	+17.0
Inland	832.3	867.5	-4.1	847.1	867.5	-2.4	911.0	867.5	+5.0	1023.2	867.9	+17.9

In addition to daily and monthly errors, energy stakeholders use the yearly solar radiation energy averages to evaluate the existing energy systems and plan new projects. Estimated yearly radiation gives an insight into the total production of such systems and can be compared with the yearly consumption to increase efficiency of such systems. Table 3 shows yearly average energy outputs in terms of estimated, observed and percentage error. The yearly energy averages were calculated by integrating the daily averages of the datasets. The gaps in CLARA, SARAH and ground-measured data are filled by using nearest-neighbour interpolation. The SARAH performs better than other datasets, but with CLARA following just behind. Above 65ºN, CLARA gives much lower deviations than ERA5 and ASR, while SARAH has no coverage. It can be observed from the table that ERA5 performs better at inland locations while other datasets perform better at coastal regions. It has been documented that satellite estimation methods deteriorate over snow-covered surfaces. In Norway, usually inland locations have a higher snow-depth than the coastal regions. Because of the shortcoming of satellite estimation algorithm in the differentiation of clouds from snow covers, satellite-based data do not perform as well in snow-covered areas as on snow-free areas. However, both satellite-based datasets underestimated the energy as shown by a previous study (Babar et al., 2018), while the reanalyses are observed to be overestimating. ERA5 overestimates the energy production much more at locations above 65ºN than below; other datasets give very similar deviations in energy averages at different locations. The results of this analysis shows that below 65ºN latitude, the SARAH performance is better than that of the other data sets. In addition to higher spatial and temporal resolution, the errors in this dataset are low. Above 65ºN, only CLARA gives reasonable errors.

Analysis of yearly averaged GHI in terms of RMSD, MAD and MBD is shown in appendix D. For the yearly averages, high errors are observed in ASR when all locations are taken into account, while CLARA, SARAH, and ERA5 give considerably lower errors. CLARA is observed to perform better at coastal locations than in the inland regions, while the errors increase at locations above 65ºN. SARAH has no coverage above 65ºN, and the deviations are larger at inland regions than at the coast. ERA5 provides similar errors as those of CLARA in inland, above

65ºN and below 65ºN, but shows high errors in coastal regions. CLARA performs better than ERA5 at coastal regions, because the surface radiation calculation in CLARA is made at a much finer resolution (0.05º) than in ERA5, and therefore, takes into account the changing surface conditions of the coastal regions to a larger degree. ASR on the other hand gives the highest errors among the datasets for all locations.

A seasonal analysis of the datasets is performed by dividing a typical year into 4 parts, where February to April are grouped in FMA, May to July are grouped in MJJ, August to October are grouped in ASO and November to January are grouped in NDJ. This division into seasons is made so that summer solstice is approximately in the middle of the summer season. Table E1 in appendix E illustrates the seasonal error analysis of the datasets and it shows that the RMSD values are high in FMA, and decreases as the year progresses. ASR is observed to have high monthly and daily RMSD. MAD values in the table show that monthly mean values are similar for CLARA, SARAH, and ERA5 while ASR gives considerably larger MAD. MBD shows that both reanalyses overestimate solar radiation and satellite methods mostly underestimate it. In this analysis, SARAH, CLARA, and ERA5 perform similarly and better than ASR. Moreover, there are larger errors in satellite methods than reanalyses in FMA and MJJ, mostly because of the presence of snow covers, which are difficult to differentiate from clouds in such methods (Babar et al., 2018). Low solar elevation angles at high latitude locations make this differentiation further challenging. On the contrary, ERA5 performs better than satellite datasets in FMA and NDJ at high latitudes. However, the performance of satellite methods improves in summer and autumn months.

4.1 Evaluation of different sky conditions

To evaluate the datasets for their performances in different sky conditions, the datasets were divided into clear-sky, intermediate-cloudiness, and overcast categories. This division is established based on the clear-sky index (*Kc*), which is defined as the ratio of GHI recorded on the ground to the clear-sky GHI. The BIRD clear-sky model is used to calculate the clear-sky values at the ground measurement locations (Bird and Hulstrom, 1981). After calculating clear-sky index, *Kc*, following Smith et al. (2017) and Widén et al. (2017), values higher than 0.8 are considered indicating a clear-sky day, values of *Kc* between 0.4 and 0.8 are considered as intermediate-cloudy and values below 0.4 are considered as overcast.

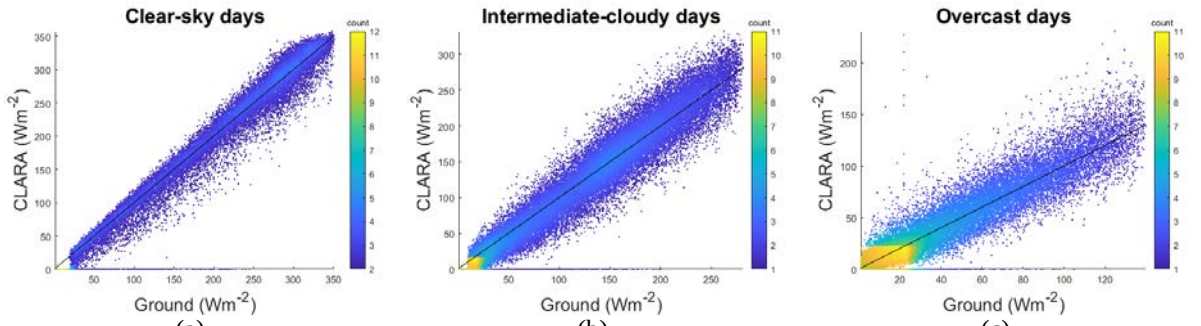

(a) (b) (c)

CLARA	RMSD (Wm^{-2})	MAD (Wm^{-2})	MBD (Wm^{-2})
Clear-sky	21.5	13.8	-4.0
Intermediate-cloudiness	22.1	16.0	-3.3
Overcast	12.8	8.7	-0.2

Figure 3: CLARA daily averaged errors under clear-sky, intermediate-cloudiness, and overcast categories. Scatter plots for the different sky-categories are shown. The coloured legend bar shows the density of points in the scatter plot.

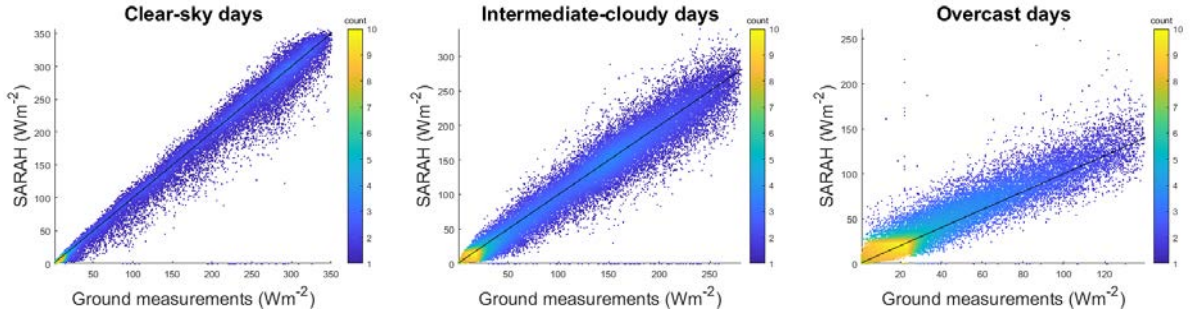

(a) (b) (c)

SARAH	RMSD (Wm^{-2})	MAD (Wm^{-2})	MBD (Wm^{-2})
Clear-sky	20.4	12.8	-5.5
Intermediate-cloudiness	20.2	13.5	-3.0
Overcast	13.2	8.7	4.4

Figure 4: As Figure 3, but for SARAH.

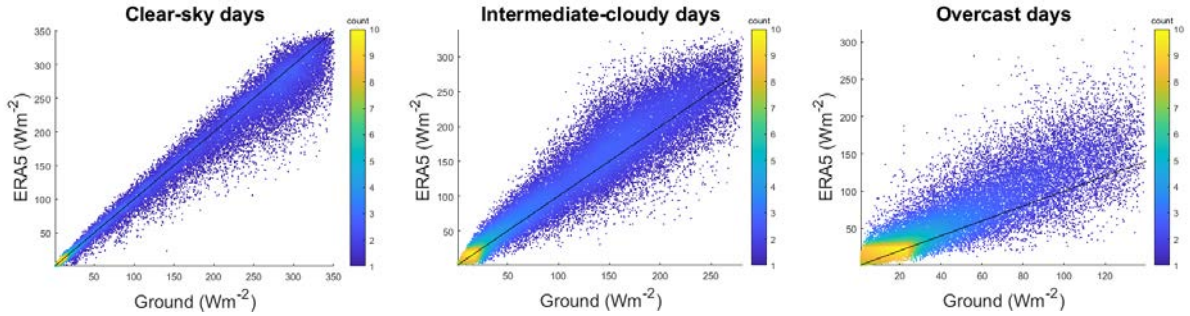

(a) (b) (c)

ERA5	RMSD (Wm^{-2})	MAD (Wm^{-2})	MBD (Wm^{-2})
Clear-sky	25.5	16.8	-10.0
Intermediate-cloudiness	28.5	19.9	8.7
Overcast	29.6	18.6	15.2

Figure 5: As Figure 3, but for ERA5.

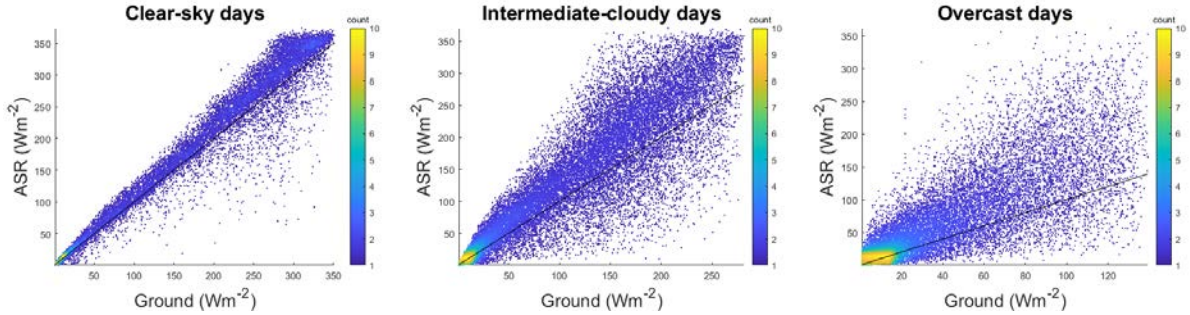

(a) (b) (c)

ASR	RMSD (Wm^{-2})	MAD (Wm^{-2})	MBD (Wm^{-2})
Clear-sky	29.2	21.1	11.6
Intermediate-cloudiness	51.3	37.2	23.3
Overcast	49.0	30.8	25.0

Figure 6: As Figure 3, but for ASR.

Figure 3-6 show the results of cloudiness classification of the datasets. Overall in the three categories, SARAH performs better than other datasets while ASR performs the worst. In clear-sky category, an underestimation is observed in SARAH, CLARA, and ERA5, while ASR overestimates radiation. CLARA performs slightly worse than SARAH in this category, but both have the same correlation coefficients of 0.98, while ERA5 and ASR both have a correlation of 0.97. Similarly, in the intermediate-cloudy category, both satellite databases underestimate, while reanalyses overestimate. Finally, in the overcast category, CLARA slightly underestimates solar radiation while other datasets overestimate. In this category, SARAH and CLARA are found to perform very similar with correlation coefficients of 0.95 and 0.94, respectively. It should be noted that the sky cloudiness differentiation is

performed on the basis of a clear-sky model and ground observed GHI. In conclusion, all the models have discrepancies in presenting clouds in all types of sky conditions.

As explained in Section 2, under clear-sky conditions CLARA uses aerosol information from Global Aerosol Data Set/Optical Properties of Aerosols and Clouds (GADS/OPAC) climatology and integrated water-vapour information from ERA-interim, and SARAH uses both Monitoring Atmospheric Composition and Climate (MACC climatology) and integrated water-vapour from ERA-Interim. Aerosol information from MACC climatology is observed to have higher accuracy than GADS/OPAC climatology (Mueller and Träger-Chatterjee, 2014). The maximum aerosol optical depth (AOD) is reduced in GADS/OPAC climatology for the CLARA dataset, but the results show that the climatology used in SARAH performs better than in CLARA even after the modifications. The negative biases observed in the clear-sky and intermediate-cloudy categories are possibly due to incorrect prediction of clouds and the aerosol climatology being too thick, which results in an underestimation of solar radiation. As reported in Mueller and Träger-Chatterjee (2014) and Polo et al. (2014), both MACC and GADS/OPAC climatologies result in underestimation of surface solar radiation because of the apparent overestimation in AOD thickness. In addition to aerosol optical depth, vertically-integrated water vapour values taken from ERA-Interim are shown to be too large (Kishore et al., 2011), which can further attenuate the surface solar radiation. Moreover, monthly mean values of aerosol optical depths are used which might also cause errors for daily resolutions. In ERA5, the radiative transfer model RTTOV11 (Radiative Transfer for TOVS) has a tendency to underestimate reflectance of high cumulus cloud tops while the reflectance of lower water clouds is overestimated. These cloud top reflectance errors possibly result in an underestimation in clear-sky conditions and overestimation in intermediate-cloudy and overcast conditions. In ASR, all the conditions are overestimated which shows that there is an underestimation in aerosol optical depth and cloudiness in the atmosphere.

After analysing different sky conditions, it can be concluded that estimations based solely on satellite retrievals generally provide a much better result. However, SARAH is limited to 60-65ºN (in Scandinavia) and CLARA is limited to daily and monthly means. For high latitude and high recording frequency, ERA5 can still provide an alternative, especially for clear-sky and intermediate-cloudy conditions in cases where satellite coverage is not available or have missing data.

4.2 Analysis of daily average TCWC and daily sky-condition classification in ERA5

To analyse the cloud placement of ERA5, the total cloud water content (TCWC) and short wave solar radiation downward, clear-sky (SWSDC) from ERA5 are used here. To obtain TCWC, total column liquid condensate and total column ice condensate from ERA5 were added together. ERA5 and other reanalyses have an overestimation or a positive bias in solar radiation as documented here and in accordance with Urraca et al. (2017b) and Urraca et al. (2018). On the contrary, satellite methods have a negative bias but higher accuracy (Riihelä et al., 2015). Reanalyses are based on weather-prediction models, and although assimilation of observations to some extent constrains these models, the weather patterns of the reanalysis may still be out of phase with reality. A small misrepresentation of clouds in space and time may have a large impact on the high-frequency correlation between model and *in-situ* observations, with regard to radiative fluxes such as solar radiation, and hereby large RMSD are induced. However at longer time scales, *i.e.* monthly or yearly time scales, the reanalysis may represent cloud frequency to a satisfactory degree because large errors in daily averages are compensated for in the seasonal mean, implying that reanalysis becomes a valuable alternative for estimating local solar resources. This can be observed by comparing the daily and monthly RMSD of ERA5 with satellite based datasets in table 2. For all the locations, the RMSD of monthly values for ERA5 is similar to that of CLARA and SARAH, but the RMSD of daily values (in parentheses) is considerably larger in ERA5 as compared to the satellite databases. On even longer time scales the difference decreases further, which can be observed by analysing yearly averages from table D1 in appendix D. In this section, the cloud representation in ERA5 on daily averages is explored (for years 2000 to 2015) and an analysis is given on the random errors in the presence of clouds at lower time scales. Clear-sky indices for all datasets are obtained by using SWSDC from ERA5 because the clear-sky values from ERA5 have the aerosol and water content information, which is used in calculating the surface solar radiation. The approach used in Section 4.1 is used here to classify days into the three categories by using clear-sky index, *Kc*. The analysis in this section is performed for days when the solar zenith angle is lower than 90º.

Table 4

The number of days and mean TCWC from *in-situ* ground measurements, ERA5 and CLARA are shown in the table for different sky categories. The number of days and mean TCWC in each cloudiness category for ERA5 is shown separately for cases when ERA5 and ground measurements agree on classification and for cases when there is a disagreement. Years from 2000 to 2015 are used in the analysis over all locations included in the study (see appendix B).

	Ground data		CLARA data		ERA5 data		ERA and ground agree		ERA and ground disagree	
	No. of days	Mean TCWC ($Kg.m^{-2}$)	No. of days	Mean TCWC ($Kg.m^{-2}$)	No. of days	Mean TCWC ($Kg.m^{-2}$)	No. of days	Mean TCWC ($Kg.m^{-2}$)	No. of days	Mean TCWC ($Kg.m^{-2}$)
Clear-sky	38265 (30.2 %)	0.03	39516 (31.3%)	0.03	53211 (33.4%)	0.02	29500	0.02	8765	0.07
Intermediate -cloudiness	49207 (38.8 %)	0.09	45244 (35.8%)	0.10	75268 (47.4%)	0.10	34700	0.10	14507	0.07
Overcast	39181 (30.9 %)	0.22	41417 (32.8%)	0.22	30389 (19.1%)	0.29	20914	0.30	18004	0.12

Table 4 shows the number of days and mean TCWC for each of the sky categories. In table 4, daily averages of solar radiation from CLARA are used to make a comparison with ERA5 in sky classification. It can be seen that ground measurement and CLARA classify almost the same percentage of days into each category even though the number of days available for these are not the same because of the missing values. CLARA also gives very similar mean TCWC values as ground measurements. On the contrary, ERA5 is observed to classify a higher number of days as intermediate-cloudy and a lower number of days as overcast than *in-situ* observations, hence showing that it has a negative bias towards classifying a day as overcast. Moreover, in ERA5 the mean TCWC is slightly underestimated in the clear-sky category but largely overestimated in overcast category. Table 4 further shows the number of days and mean TCWC for conditions when ERA5 and ground measurements agree on classification and for when there is a disagreement. Here it can be seen that the mean TCWC of days with agreement is the same as that of ERA5, but on the days of disagreement, there is an overestimation in mean TCWC in clear-sky days and an underestimation in overcast days. These results show that on clear-sky days, ERA5 has more clouds than *in-situ* observations, which is seen by higher levels of TCWC, while on the overcast days there are a lower amount of clouds, which is seen by lower levels of TCWC. However, it can be seen from the table that in clear-sky category, ERA5 and ground-measurements agree 77% of the time. The agreement on sky-condition is smaller in intermediate-cloudy category where 41% of the time ERA5 predicts the same conditions as *in-situ* observations, while the agreement in overcast category is 53%. Overall, 67.3% of the times it is seen that ERA5 and ground measurements classify the same conditions. Figure 7 shows the scatter plot of ground measurements and ERA5 for both of these conditions, when there is an agreement on classification and when there is a disagreement. It can be seen that the spread is large when there is a disagreement. A correlation coefficient of 0.98 is found for agreement data points while a correlation coefficient of 0.90 is found for disagreement point.

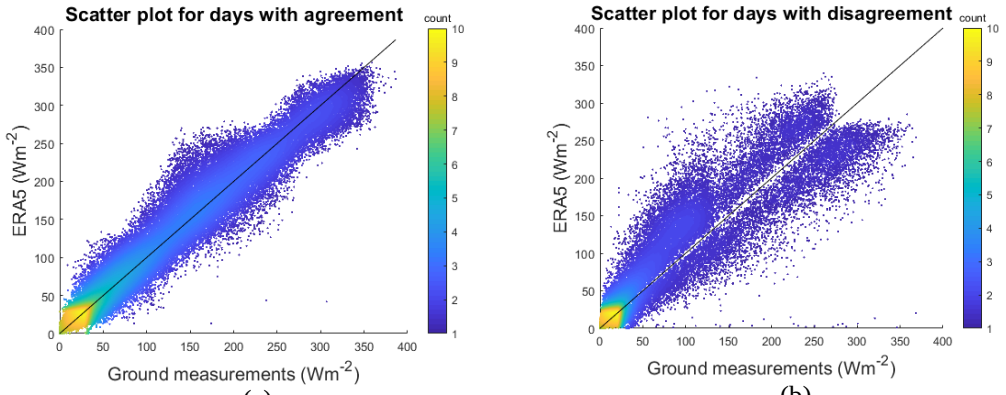

Figure 7: Scatter plots for the days when ERA5 and ground measurement agree in classification and when there is a disagreement. A correlation coefficient of 0.98 is found for agreement points and 0.90 for disagreement points.

Table 5 illustrates RMSD, MAD, and MBD of ERA5 in different sky categories. It shows the error metrics for the days when ERA5 and ground measurements agree on a category and for when there is a disagreement. The days of agreement on sky categories in table 5 can be compared to the deviations presented in Section 4.1, Figure 3. It can be seen that on the days of agreement ERA5 performs very similar to CLARA. However, large errors are observed when ERA5 does not agree with ground measurements in sky categorization. In terms of RMSD and MAD, the highest increase is seen in clear-sky and overcast categories. The MBD is positive in clear-sky category and negative in intermediate-cloudiness and overcast categories, which again shows that there are less amount of clouds in the clear-sky category and more clouds in intermediate-cloudiness and overcast categories. From a solar energy-harvesting point of view, the clear-sky days produce more energy than intermediate-cloudy or overcast days. It can be observed that ground-measurement and ERA5 predicts almost the same percentage of clear-sky days, which further shows that on daily averages reanalyses may not predict clouds accurately but on longer time scales, the solar radiation estimation improves.

Table 5

RMSD, MAD, and MBD for ERA5 daily averages in different sky categories. The errors are shown for the days when ERA5 and ground measurements agree on classification and for when they do not agree. Years from 2000 to 2015 are used in the analysis over all locations included in the study (see appendix B).

	Agreement on sky conditions			Disagree on sky conditions		
	RMSD (Wm^{-2})	MAD (Wm^{-2})	MBD (Wm^{-2})	RMSD (Wm^{-2})	MAD (Wm^{-2})	MBD (Wm^{-2})
Clear-sky	16.9	11.8	5.6	42.9	31.2	31.2
Intermediate-cloudiness	25.7	17.7	-7.4	33.8	24.2	-15.1
Overcast	15.3	9.6	-4.5	38.4	26.3	-26.3

5. Conclusion

This study provides a comprehensive evaluation of different GHI estimating datasets for high-latitude locations. Overall, SARAH provides lower errors than other datasets but is limited to 60-65ºN latitudes in Scandinavia; hence, it cannot provide complete coverage on the northern Scandinavian locations. For monthly averages of GHI, MAD of 5.8 Wm^{-2} is found for SARAH. Nevertheless, it provides very high quality solar-radiation estimates for the area it covers. The second best dataset found in this study is CLARA that has a global coverage and provides multi-decadal time series. For monthly mean estimates of GHI, CLARA gives a MAD of 6.3 Wm^{-2}. One of the challenges for estimating GHI at high latitude locations is the ability of the satellite estimation algorithms to differentiate between clouds and snow covers. ERA5 being a coarse-resolution global dataset is observed to perform nearly as well as CLARA with a MAD of 6.4 Wm^{-2} for monthly averages of GHI. ERA5 has similar spatial resolution as CLARA but it provides data on higher temporal resolutions and unlike CLARA, it has no missing values. ASR is found to have the highest errors in this analysis. MAD of 14.5 Wm^{-2} is found for ASR monthly means. In a similar study performed by Urraca et al. (2017b), MAD of 8 – 13 Wm^{-2} was reported for CM-SAF daily means datasets.

Both satellite estimation and reanalyses have problems in estimating solar radiation in intermediate-cloudiness and overcast conditions. To evaluate the strength of the datasets, the ground-measured data is divided into clear-sky, intermediate-cloudiness, and overcast categories and error statistics are calculated. In this test, satellite based estimations perform better than reanalyses. However, ERA5 has larger errors than CLARA and SARAH, but still considerably smaller errors than ASR. At high latitude locations, the seasonal variation in the length of the day is extreme. Taking this into consideration, an analysis is performed for different seasons. In this analysis, CLARA, SARAH and ERA5 have similar errors in the range of 6-13 Wm^{-2} in the summer months; however, ASR has relatively high errors in all seasons. On yearly GHI averages, SARAH provides the lowest MAD of 3.9 Wm^{-2}, followed by 4.8 Wm^{-2} for CLARA, 5.6 Wm^{-2} for ERA5, and 17.8 Wm^{-2} for ASR. SARAH and CLARA also provide better yearly energy estimates than ERA5 and ASR. CLARA and ERA5 are observed to provide lower errors below 65ºN than above, while CLARA and SARAH perform better at coastal regions, and ERA5 performs better in inland locations that have more snow covers.

Finally, an in-depth analysis is performed on ERA5 for its compatibility in sky stratification. It is found that in clear-sky conditions, the TCWC is overestimated, while in intermediate-cloudiness and overcast conditions it is underestimated. It is also observed that ERA5 has a positive bias on estimating clear-sky and intermediate-cloudy conditions, while a negative bias is seen in estimating overcast conditions. In conclusion, both CLARA and SARAH provide good estimates but both of these datasets have disadvantages, including the spatial limits of SARAH and the low temporal frequency of CLARA. On the other hand, ERA5 provides advantages in the form of historical data series and global coverage. On the basis of these results it is suggested that CLARA and SARAH provides better estimates for solar radiation, but ERA5 can be used to fill the missing data in these datasets.

Acknowledgements

We would like to thank NIBIO, ECMWF and CM-SAF for providing the data used in this study. This work is supported by Troms county and industry development fund under the project title, "Renewable energy in the arctic - academy and business in a joint effort" RDA12/46. Data was partly processed at the Stallo supercomputer at the University of Tromsø (UiT) provided by Norwegian Metacenter for Computational Science (NOTUR), project no.: NN9348k.

Appendix A

Table A1

Locations of the Norwegian measurement stations analysed in this study.

	Station	Latitude	Longitude	Altitude	Land type
1	Holt	69.65	18.91	12	Coastal
2	Sortland	68.65	15.28	14	Coastal
3	Vågønes	67.28	14.45	26	Coastal
4	Tjøtta	65.83	12.43	10	Coastal
5	Skogmo	64.51	12.02	32	Inland
6	Rissa	63.59	9.97	23	Coastal
7	Kvithamar	63.49	10.88	28	Inland
8	Skjetlein	63.34	10.3	44	Coastal
9	Surnadal	62.98	8.69	5	Inland
10	Tingvoll	62.91	8.19	23	Coastal
11	Fåvgang	61.46	10.19	184	Inland
12	Fureneset	61.29	5.04	12	Coastal
13	Gausdal	61.22	10.26	375	Inland
14	Løken	61.12	9.06	527	Inland
15	Ilseng	60.8	11.2	182	Inland
16	Kise	60.77	10.81	129	Inland
17	Apelsvoll	60.7	10.87	262	Inland
18	Hønefoss	60.14	10.27	126	Inland
19	Årnes	60.13	11.39	162	Inland
20	Etne	59.66	5.95	8	Inland
21	Ås	59.66	10.78	94	Inland
22	Bø	59.42	9.03	105	Inland
23	Rakkestad	59.39	11.39	102	Inland
24	Ramnes	59.38	10.24	39	Coastal
25	Tomb	59.32	10.81	12	Coastal
26	Gjerpen	59.23	9.58	41	Coastal
27	Hjelmeland	59.23	6.15	43	Inland
28	Tjølling	59.05	10.13	19	Coastal
29	Særheim	58.76	5.65	90	Coastal
30	Landvik	58.34	8.52	10	Coastal
31	Lyngdal	58.13	7.05	4	Inland

548 **Appendix B**

549 **Table B1**

550 List of years not included in the study.

	Station	Years having more than 5% missing data	Years failing Long and Dutton test	Years having operational error (snow/frost/ shading/soiling)	Years having equipment error
1	Holt	2001,2002,2006,2007,2008,2010	2013		2000
2	Sortland	2000,2006,2007,2010,2013			
3	Vågønes	2006,2007		2002	
4	Tjøtta	2006,2007			2008, 2012
5	Skogmo	2006,2007,2008,2015		2011	2013, 2014
6	Rissa	2006,2007	2000		
7	Kvithamar	2006,2007,2013			
8	Skjetlein	2006,2007	2000		
9	Surnadal	2006,2007,2014			
10	Tingvoll	2006,2007,2012			
11	Fåvang	2006,2007			2001
12	Fureneset	2006,2007,2011,2012			
13	Gausdal	2006,2007,2009			2015
14	Løken	2006,2007			
15	Ilseng	2006,2007,2004	2000	2009	
16	Kise	2002,2006,2007,2015		2013	
17	Apelsvoll	2006,2007		2002,2003,2004	2009
18	Hønefoss	2006,2007	2000		
19	Årnes	2006,2007			
20	Etne	2006,2007		2004,2012	
21	Ås	2006,2007			
22	Bø	2000,2006,2007			
23	Rakkestad	2006,2007			
24	Ramnes	2006,2007		2009	
25	Tomb	2006,2007	2009		
26	Gjerpen	2006,2007,2015			
27	Hjelmeland	2006,2007			2002, 2015
28	Tjølling	2006,2007,2008,2014		2012,2015	2009, 2010
29	Særheim	2000,2006,2007			
30	Landvik	2006,2007		2005,2010,2014, 2015	
31	Lyngdal	2006,2007	2001		

551

552

Appendix C

Table C1

Error metrics expressed in Wm^{-2}, for the datasets analysed in this study. Number without parentheses are monthly averaged errors while in parentheses are daily averaged errors.

Station	RMSD(Wm^{-2})				MAD(Wm^{-2})				MBD(Wm^{-2})			
	CLARA	SARAH	ERA5	ASR	CLARA	SARAH	ERA5	ASR	CLARA	SARAH	ERA5	ASR
Holt	5.5 (9.1)	-	4.7 (12.0)	9.6 (18.8)	1.5 (2.9)	-	1.1 (3.5)	2.8 (4.8)	-1.5 (-1.4)	-	1.1 (1.4)	2.5 (3.4)
Sortland	17.5 (23.0)	-	12.5 (29.9)	15.1 (38.2)	11.4 (16.0)	-	7.7 (18.9)	9.7 (24.4)	-11.0 (-12.0)	-	1.1 (2.4)	0.6 (2.2)
Vågønes	5.1 (13.8)	-	10.4 (26.7)	20.9 (42.1)	3.2 (8.7)	-	5.7 (15.0)	12.8 (24.8)	-0.7 (0.3)	-	3.9 (6.3)	11.8 (16.2)
Tjøtta	6.1 (13.8)	-	12.8 (29.2)	27.8 (47.9)	4.6 (9.5)	-	8.4 (17.4)	16.9 (28.0)	-0.3 (1.3)	-	7.9 (10.7)	15.2 (19.4)
Skogmo	12.4 (20.0)	11.8 (20.8)	8.2 (23.6)	20.2 (41.6)	7.8 (13.3)	8.2 (13.4)	5.3 (14.2)	12.5 (25.8)	-3.7 (-2.4)	-6.3 (-5.6)	1.0 (2.5)	11.4 (15.3)
Rissa	8.2 (17.3)	7.2 (17.6)	8.2 (27.1)	24.1 (45.4)	5.5 (12.3)	4.9 (11.5)	5.1 (17.1)	14.8 (27.7)	-2.7 (-1.5)	-3.3 (-2.4)	2.1 (4.2)	13.6 (19.5)
Kvithamar	7.3 (16.0)	7.8 (16.8)	7.7 (26.4)	31.6 (47.7)	5.1 (11.4)	1.0 (10.6)	5.2 (16.4)	20.3 (29.5)	-2.4 (-1.2)	-0.2 (-4.4)	-0.1 (1.4)	19.2 (23.1)
Skjetlein	7.9 (17.4)	8.8 (17.6)	7.2 (25.9)	29.9 (46.5)	6.0 (12.7)	6.4 (11.6)	5.1 (16.5)	19.7 (28.6)	-1.0 (0.8)	-6.0 (-4.8)	0.4 (2.0)	18.9 (22.6)
Surnadal	9.7 (20.8)	11.1 (23.5)	10.9 (28.4)	19.0 (41.2)	7.0 (14.1)	7.7 (14.5)	7.5 (17.9)	12.9 (25.2)	-4.1 (-2.7)	-6.0 (-5.1)	6.5 (8.3)	11.9 (14.8)
Tingvoll	8.3 (18.0)	9.3 (20.0)	10.4 (27.1)	16.9 (40.0)	6.4 (13.4)	6.4 (12.6)	6.5 (16.9)	10.7 (24.5)	-1.7 (-0.1)	-4.8 (-4.0)	5.1 (7.0)	8.4 (11.1)
Fåvang	13.1 (22.3)	10.0 (18.8)	10.4 (27.3)	21.2 (43.9)	9.5 (16.3)	7.3 (12.8)	6.8 (18.0)	14.6 (29.2)	-8.4 (-7.6)	-6.8 (-6.6)	1.8 (2.8)	14.1 (19.5)
Fureneset	4.7 (14.9)	5.7 (16.8)	10.7 (28.3)	18.5 (42.0)	3.5 (10.4)	3.8 (9.2)	6.9 (17.0)	12.6 (26.3)	-1.1 (0.6)	-2.8 (-1.8)	6.4 (8.6)	11.3 (14.1)
Gausdal	11.4 (20.6)	7.0 (17.4)	13.2 (27.7)	20.9 (42.6)	8.8 (15.3)	5.2 (12.1)	8.8 (18.3)	14.8 (29.0)	-1.2 (0.4)	-1.9 (-0.6)	5.1 (7.1)	14.6 (17.9)
Løken	14.3 (24.3)	10.7 (21.0)	9.2 (28.3)	12.7 (40.5)	9.5 (17.6)	7.4 (14.5)	5.9 (18.6)	8.2 (26.6)	-8.4 (-7.2)	-6.7 (-6.1)	1.8 (4.0)	3.7 (6.1)
Ilseng	11.8 (23.4)	9.3 (19.2)	11.0 (28.0)	21.4 (43.9)	8.8 (16.8)	5.8 (12.9)	7.6 (18.7)	16.7 (29.7)	-5.9 (-4.1)	-2.2 (-1.0)	-1.1 (1.0)	16.7 (19.8)
Kise	9.9 (20.6)	8.3 (18.2)	8.9 (25.9)	22.6 (42.7)	6.8 (15.1)	5.5 (12.4)	6.0 (17.0)	16.1 (28.6)	-1.0 (0.9)	-1.5 (0.4)	2.3 (4.3)	16.1 (20.8)
Apelsvoll	10.2 (19.6)	8.4 (17.4)	9.1 (25.8)	31.8 (48.2)	7.7 (14.7)	5.0 (11.9)	6.3 (17.3)	25.0 (34.0)	1.6 (4.2)	-0.2 (1.5)	2.8 (5.1)	25.0 (29.0)
Hønefoss	7.0 (16.6)	7.1 (15.8)	8.9 (25.7)	20.8 (41.6)	5.3 (12.2)	4.8 (10.8)	6.1 (17.0)	15.2 (28.0)	-3.3 (-1.3)	-3.5 (-2.2)	-0.1 (2.0)	15.1 (20.3)
Årnes	9.0 (17.3)	7.8 (16.2)	7.9 (24.6)	19.8 (40.0)	6.2 (12.7)	5.1 (11.0)	5.2 (16.3)	14.9 (26.6)	-4.0 (-2.8)	-3.8 (-3.0)	-1.3 (0.1)	13.3 (18.4)
Etne	9.3 (20.0)	9.7 (22.0)	12.8 (29.4)	23.1 (48.6)	6.9 (14.5)	7.0 (14.8)	8.9 (19.6)	15.0 (31.0)	-4.4 (-2.9)	-5.4 (-4.6)	6.4 (8.9)	14.5 (19.4)
Ås	7.3 (13.6)	7.1 (14.6)	8.0 (24.5)	21.1 (41.0)	4.8 (8.7)	5.1 (10.0)	5.3 (16.1)	15.1 (26.7)	-3.5 (-1.9)	-4.0 (-2.8)	-2.1 (-0.5)	14.4 (19.2)
Bø	7.9 (17.8)	6.5 (16.6)	10.3 (25.4)	21.5 (43.2)	5.7 (13.0)	4.6 (11.6)	7.1 (17.1)	16.4 (29.4)	1.4 (3.0)	1.5 (3.0)	4.9 7.5)	16.2 (20.3)
Rakkestad	7.2 (15.9)	7.8 (17.8)	8.2 (26.1)	21.0 (40.6)	5.5 (11.5)	5.5 (10.3)	5.8 (16.4)	16.1 (27.2)	-2.9 (-1.4)	-4.3 (-3.6)	0.6 (2.5)	15.2 (18.3)
Ramnes	8.9 (16.7)	7.5 (15.4)	8.2 (24.0)	22.1 (40.8)	7.1 (12.3)	5.5 (10.6)	5.8 (15.8)	16.4 (26.5)	-5.6 (-4.1)	-3.4 (-2.0)	-1.3 (0.3)	15.8 (18.7)
Tomb	11.5 (19.0)	12.7 (19.0)	11.2 (28.0)	20.3 (40.9)	7.0 (12.8)	8.9 (14.0)	6.9 (17.7)	14.4 (25.6)	-5.9 (-4.5)	-5.0 (-3.9)	-3.3 (-2.1)	12.5 (16.9)
Gjerpen	11.5 (19.1)	8.8 (19.9)	11.6 (25.8)	20.4 (40.8)	8.3 (14.5)	1.1 (14.3)	8.4 (18.1)	14.8 (27.9)	-4.3 (-3.0)	-0.2 (-4.1)	-1.3 (0.3)	10.7 (15.4)
Hjelmeland	4.7 (16.6)	5.5 (16.1)	10.9 (29.5)	19.7 (46.0)	3.4 (12.1)	3.6 (10.9)	7.5 (19.6)	13.9 (31.1)	-0.1 (1.6)	-0.9 (0.2)	6.6 (9.8)	13.5 (18.1)
Tjølling	8.2 (18.0)	7.5 (13.8)	11.4 (26.5)	28.5 (45.1)	6.0 (12.8)	5.2 (9.6)	7.5 (16.8)	19.7 (29.6)	-0.1 (1.9)	-1.9 (-0.6)	4.4 (7.2)	19.1 (25.1)
Særheim	5.9 (15.2)	6.2 (16.0)	7.4 (26.4)	17.0 (43.5)	4.4 (10.8)	4.3 (10.8)	4.9 (16.7)	11.6 (28.0)	-1.2 (0.3)	-1.9 (-0.7)	2.2 (4.1)	9.7 (12.8)
Landvik	7.3 (16.5)	6.3 (14.3)	10.2 (25.7)	23.0 (42.2)	5.2 (11.6)	4.6 (9.7)	6.5 (16.7)	15.8 (28.1)	1.2 (3.9)	-0.4 (1.8)	5.5 (8.8)	15.5 (21.3)
Lyngdal	11.3 (21.8)	9.6 (22.8)	12.1 (29.9)	15.8 (41.5)	7.4 (13.7)	1.2 (13.5)	8.3 (19.5)	10.9 (25.9)	-6.0 (-6.1)	-0.4 (-1.8)	2.9 (3.6)	5.9 (7.0)

APPENDIX D

Table D1

Statistical errors of the yearly average solar radiation for the datasets included in the study. This table shows the deviations for inland, coastal, above 65 ° N, and below 65ºN latitude regions. RMSD, MAD, and MBD are expressed in Wm^{-2}.

	RMSD ($Wm^{-2}year^{-1}$)				MAD ($Wm^{-2}year^{-1}$)				MBD ($Wm^{-2}year^{-1}$)			
	CLARA	SARAH	ERA5	ASR	CLARA	SARAH	ERA5	ASR	CLARA	SARAH	ERA5	ASR
All Sites	7.4	5.2	6.8	18.7	4.8	3.9	5.6	17.8	-4.2	-2.8	4.4	17.5
Above 65ºN	8.9	-	9.6	16.6	5.2	-	8.8	15.6	-4.4	-	7.1	13.4
Below 65ºN	7.2	5.2	6.4	18.9	4.8	3.9	5.2	18.1	-4.1	-2.9	4.1	18.0
Coastal	6.2	4.9	7.4	18.1	3.8	3.5	6.2	17.1	-3.1	-2.4	4.6	16.6
Inland	8.2	5.4	6.4	19.2	5.6	4.0	5.0	18.4	-5.0	-3.0	4.2	18.2

Appendix E

Table E1

Seasonal analysis of the datasets showing the variations in terms of RMSD, MAD, and MBD and expressed in Wm^{-2}. CLARA and SARAH performs similarly and better than other datasets, while ERA5 gives median values and ASR performs the worst

	RMSD (Wm^{-2})				MAD (Wm^{-2})				MBD (Wm^{-2})			
	FMA	MJJ	ASO	NDJ	FMA	MJJ	ASO	NDJ	FMA	MJJ	ASO	NDJ
CLARA	12.7 (29.0)	9.4 (22.3)	8.4 (16.6)	1.9 (13.1)	8.8 (17.3)	7.3 (17.0)	6.4 (11.5)	0.5 (7.9)	-7.6 (-11.7)	1.1 (1.3)	-4.1 (0.4)	-0.3 (-7.1)
SARAH	12.3 (21.9)	9.8 (25.5)	8.8 (15.9)	5.5 (10.2)	9.2 (15.0)	7.8 (17.9)	6.8 (11.0)	3.5 (4.8)	-7.4 (-7.2)	-2.8 (-3.1)	-4.0 (1.2)	-2.9 (-2.4)
ERA5	11.5 (23.8)	15.1 (41.3)	9.9 (24.1)	4.7 (9.7)	8.8 (17.0)	12.2 (31.8)	7.5 (17.0)	2.7 (4.5)	6.9 (7.3)	7.3 (7.3)	-3.1 (2.2)	-0.1 (0.4)
ASR	22.5 (35.9)	38.4 (67.6)	17.0 (38.6)	5.5 (11.3)	19.4 (26.0)	34.6 (52.8)	12.8 (27.1)	3.4 (5.8)	18.9 (19.9)	34.0 (34.2)	9.2 (14.3)	1.2 (1.5)

References

Babar, B., Graversen, R., Boström, T., 2018. Evaluating CM-SAF solar radiation CLARA-A1 and CLARA-A2 datasets in Scandinavia. Solar Energy 170, 76-85.

Bird, R.E., Hulstrom, R.L., 1981. Simplified clear sky model for direct and diffuse insolation on horizontal surfaces. Solar Energy Research Inst., Golden, CO (USA).

Boilley, A., Wald, L., 2015. Comparison between meteorological re-analyses from ERA-Interim and MERRA and measurements of daily solar irradiation at surface. Renewable Energy 75, 135-143.

Bojanowski, J.S., Vrieling, A., Skidmore, A.K., 2014. A comparison of data sources for creating a long-term time series of daily gridded solar radiation for Europe. Solar Energy 99, 152-171.

Bromwich, D., Wilson, A., Bai, L., Liu, Z., Barlage, M., Shih, C.-F., Maldonado, S., Hines, K., Wang, S.-H., Woollen, J., 2017. The Arctic System Reanalysis Version 2. Bulletin of the American Meteorological Society(2017).

Cano, D., Monget, J.-M., Albuisson, M., Guillard, H., Regas, N., Wald, L., 1986. A method for the determination of the global solar radiation from meteorological satellites data. Solar energy 37(1), 31-39.

Crabtree, G., Misewich, J., Ambrosio, R., Clay, K., DeMartini, P., James, R., Lauby, M., Mohta, V., Moura, J., Sauer, P., 2011. Integrating renewable electricity on the grid, AIP Conference Proceedings. AIP, pp. 387-405.

Dee, D.P., Uppala, S.M., Simmons, A., Berrisford, P., Poli, P., Kobayashi, S., Andrae, U., Balmaseda, M., Balsamo, G., Bauer, d.P., 2011. The ERA-Interim reanalysis: Configuration and performance of the data assimilation system. Quarterly Journal of the royal meteorological society 137(656), 553-597.

ECMWF, 2018. ERA5 data documentation.

Gautier, C., Diak, G., Masse, S., 1980. A simple physical model to estimate incident solar radiation at the surface from GOES satellite data. Journal of Applied meteorology 19(8), 1005-1012.

Gueymard, C.A., 2011. Uncertainties in modeled direct irradiance around the sahara as affected by aerosols: Are current datasets of bankable quality? Journal of Solar Energy Engineering 133(3), 031024.
Hall, I.J., Prairie, R., Anderson, H., Boes, E., 1978. Generation of a typical meteorological year. Sandia Labs., Albuquerque, NM (USA).
Hammer, A., Heinemann, D., Hoyer, C., Kuhlemann, R., Lorenz, E., Müller, R., Beyer, H.G., 2003. Solar energy assessment using remote sensing technologies. Remote Sensing of Environment 86(3), 423-432.
Hans, H., Dick, D., 2016. ERA5 reanalysis is in production. https://www.ecmwf.int/en/newsletter/147/news/era5-reanalysis-production.
Heinemann, D., Lorenz, E., Girodo, M., 2006. Forecasting of solar radiation. Solar energy resource management for electricity generation from local level to global scale. Nova Science Publishers, New York.
Huld, T., Paietta, E., Zangheri, P., Pinedo Pascua, I., 2018. Assembling Typical Meteorological Year Data Sets for Building Energy Performance Using Reanalysis and Satellite-Based Data. Atmosphere 9(2), 53.
Ineichen, P., 2014. Long term satellite global, beam and diffuse irradiance validation. Energy Procedia 48, 1586-1596.
Juruš, P., Eben, K., Resler, J., Krč, P., Kasanický, I., Pelikán, E., Brabec, M., Hošek, J., 2013. Estimating climatological variability of solar energy production. Solar Energy 98, 255-264.
Karlsson, K.-G., Anttila, K., Trentmann, J., Stengel, M., Meirink, J.F., Devasthale, A., Hanschmann, T., Kothe, S., Jääskeläinen, E., Sedlar, J., 2017. CLARA-A2: the second edition of the CM SAF cloud and radiation data record from 34 years of global AVHRR data. Atmospheric Chemistry and Physics 17(9), 5809.
Kennedy, A.D., Dong, X., Xi, B., Xie, S., Zhang, Y., Chen, J., 2011. A comparison of MERRA and NARR reanalyses with the DOE ARM SGP data. Journal of Climate 24(17), 4541-4557.
Kishore, P., Ratnam, M.V., Namboothiri, S., Velicogna, I., Basha, G., Jiang, J., Igarashi, K., Rao, S., Sivakumar, V., 2011. Global (50 S–50 N) distribution of water vapor observed by COSMIC GPS RO: Comparison with GPS radiosonde, NCEP, ERA-Interim, and JRA-25 reanalysis data sets. Journal of Atmospheric and Solar-Terrestrial Physics 73(13), 1849-1860.
Long, C.N., Dutton, E.G., 2010. BSRN Global Network recommended QC tests, V2. x.
Mueller, R., Behrendt, T., Hammer, A., Kemper, A., 2012. A new algorithm for the satellite-based retrieval of solar surface irradiance in spectral bands. Remote Sensing 4(3), 622-647.
Mueller, R., Träger-Chatterjee, C., 2014. Brief accuracy assessment of aerosol climatologies for the retrieval of solar surface radiation. Atmosphere 5(4), 959-972.
Müller, R., Pfeifroth, U., Träger-Chatterjee, C., Trentmann, J., Cremer, R., 2015. Digging the METEOSAT treasure—3 decades of solar surface radiation. Remote Sensing 7(6), 8067-8101.
Noia, M., Ratto, C., Festa, R., 1993. Solar irradiance estimation from geostationary satellite data: II. Physical models. Solar Energy 51(6), 457-465.
Pfeifroth, U., Kothe, S., Müller, R., Trentmann, J., Hollmann, R., Fuchs, P., Werscheck, M., 2017a. Surface Radiation Data Set-Heliosat (SARAH)—Edition 2, Satellite Application Facility on Climate Monitoring. .
Pfeifroth, U., Kothe, S., Müller, R., Trentmann, J., Hollmann, R., Fuchs, P., Werscheck, M., 2017b. Surface Radiation Data Set–Heliosat (SARAH)–Edition 2, Satellite Application Facility on Climate Monitoring.
Pfeifroth, U., Sanchez-Lorenzo, A., Manara, V., Trentmann, J., Hollmann, R., 2018. Trends and Variability of Surface Solar Radiation in Europe Based On Surface- and Satellite-Based Data Records. Journal of Geophysical Research: Atmospheres, n/a-n/a.
Pinker, R., Laszlo, I., 1992. Modeling surface solar irradiance for satellite applications on a global scale. Journal of Applied Meteorology 31(2), 194-211.

Platt, C., 1983. On the bispectral method for cloud parameter determination from satellite VISSR data: Separating broken cloud and semitransparent cloud. Journal of climate and applied meteorology 22(3), 429-439.
Polo, J., Antonanzas-Torres, F., Vindel, J., Ramirez, L., 2014. Sensitivity of satellite-based methods for deriving solar radiation to different choice of aerosol input and models. Renewable energy 68, 785-792.
Posselt, R., Mueller, R., Stöckli, R., Trentmann, J., 2012. Remote sensing of solar surface radiation for climate monitoring—The CM-SAF retrieval in international comparison. Remote Sensing of Environment 118, 186-198.
Remund, J., Perez, R., Lorenz, E., 2008. Comparison of solar radiation forecasts for the USA, Proc. of the 23rd European PV Conference. Valencia, Spain.
Rigollier, C., Lefèvre, M., Wald, L., 2004. The method Heliosat-2 for deriving shortwave solar radiation from satellite images. Solar Energy 77(2), 159-169.
Riihelä, A., Carlund, T., Trentmann, J., Müller, R., Lindfors, A.V., 2015. Validation of CM SAF surface solar radiation datasets over Finland and Sweden. Remote Sensing 7(6), 6663-6682.
Smith, C.J., Bright, J.M., Crook, R., 2017. Cloud cover effect of clear-sky index distributions and differences between human and automatic cloud observations. Solar Energy 144, 10-21.
Stoffel, T., Renne, D., Myers, D., Wilcox, S., Sengupta, M., George, R., Turchi, C., 2010. Concentrating solar power. Golden: National Renewable Energy Laboratory.
Suri, M., Cebecauer, T., 2014. Satellite-based solar resource data: Model validation statistics versus user's uncertainty, ASES SOLAR 2014 Conference, San Francisco. pp. 7-9.
Tarpley, J., 1979. Estimating incident solar radiation at the surface from geostationary satellite data. Journal of Applied Meteorology 18(9), 1172-1181.
Trentmann, J., Kothe, S., 2016. Surface Radiation Products

Product User Manual. CM SAF Cloud, Albedo, Radiation dataset,

SAF/CM/DWD/PUM/GAC/RAD(2.1).
Urraca, R., Gracia-Amillo, A.M., Huld, T., Martinez-de-Pison, F.J., Trentmann, J., Lindfors, A.V., Riihelä, A., Sanz-Garcia, A., 2017a. Quality control of global solar radiation data with satellite-based products. Solar Energy 158, 49-62.
Urraca, R., Gracia-Amillo, A.M., Koubli, E., Huld, T., Trentmann, J., Riihelä, A., Lindfors, A.V., Palmer, D., Gottschalg, R., Antonanzas-Torres, F., 2017b. Extensive validation of CM SAF surface radiation products over Europe. Remote sensing of environment 199, 171-186.
Urraca, R., Huld, T., Gracia-Amillo, A., Martinez-de-Pison, F.J., Kaspar, F., Sanz-Garcia, A., 2018. Evaluation of global horizontal irradiance estimates from ERA5 and COSMO-REA6 reanalyses using ground and satellite-based data. Solar Energy 164, 339-354.
Widén, J., Shepero, M., Munkhammar, J., 2017. On the properties of aggregate clear-sky index distributions and an improved model for spatially correlated instantaneous solar irradiance. Solar Energy 157, 566-580.
Wild, M., 2008. Short-wave and long-wave surface radiation budgets in GCMs: A review based on the IPCC-AR4/CMIP3 models. Tellus A 60(5), 932-945.
Wild, M., Folini, D., Henschel, F., Fischer, N., Müller, B., 2015. Projections of long-term changes in solar radiation based on CMIP5 climate models and their influence on energy yields of photovoltaic systems. Solar Energy 116, 12-24.
Yi, Y., Kimball, J.S., Jones, L.A., Reichle, R.H., McDonald, K.C., 2011. Evaluation of MERRA land surface estimates in preparation for the soil moisture active passive mission. Journal of Climate 24(15), 3797-3816.
You, Q., Sanchez-Lorenzo, A., Wild, M., Folini, D., Fraedrich, K., Ren, G., Kang, S., 2013. Decadal variation of surface solar radiation in the Tibetan Plateau from observations, reanalysis and model simulations. Climate dynamics 40(7-8), 2073-2086.

695 Zhao, L., Lee, X., Liu, S., 2013. Correcting surface solar radiation of two data assimilation systems
696 against FLUXNET observations in North America. Journal of Geophysical Research: Atmospheres
697 118(17), 9552-9564.
698 Øyvind, B., Anne, L., Løvholm, Sonia, L., 2013. Resource mapping of solar energy an overview of
699 available data in Norway. Kjeller Vindteknikk

700 Report KVT/OB/2013/R046.

701